PHYSICAL REVIEW E **84**, 012901 (2011)

# Aerodynamic trick for visual stabilization during downstroke in a hovering bird

Jian-Yuan Su, Shang-Chieh Ting, Yu-Hung Chang, and Jing-Tang Yang
*Department of Mechanical Engineering, National Taiwan University No. 1, Sec. 4, Roosevelt Road, Taipei 10617, Taiwan*

(Received 22 February 2011; revised manuscript received 26 April 2011; published 21 July 2011)

We provide physical insight into how a small hovering bird attains stabilized vision during downstroke. A passerine generates a lift force greater than its body weight during downstroke, leading to a substantial swing of the bird body, but the bird's eyes are nearly stable. Employing digital particle-image velocimetry, we demonstrate that a hovering passerine generates a lift force acting dorsal to the center of mass, concurrently resulting in rotational and translational displacements of the bird's body. The most notable finding is that the rotational and translational displacements at the bird's eyes almost cancel each other; the displacement of the eye is ∼8% that of the trailing tip of the tail. This aerodynamic trick enables a bird to attain stabilized vision beneficial for the inspection of the environment.

DOI: 10.1103/PhysRevE.84.012901 PACS number(s): 87.85.gj, 47.32.C−, 87.19.ru, 47.63.mc

Passerines are capable of executing asymmetric hovering flight (referring to stationary flight in the air by asymmetric wingbeat) and produce lift forces for weight support during merely the downstroke [1,2]. While studying the aerodynamic mechanisms of hovering flight in a passerine, we noticed that the bird's eyes were extremely stable (i.e. stationary) during the vigorous downstroke. This unique phenomenon of stabilized vision is observable also in many small bird species. Visual stabilization is an imperative mechanism for a bird to survive because without stabilized vision to inspect the environment, any skillful flight capability is in vain [3,4]. Most authors of avian literature have discussed the stabilization of the head or eyes from a zoophysiological perspective. Birds offset and isolate perturbations (sensed by nervous system) from the head by a sophisticated musculoskeletal system, obtaining a stabilized vision [4]. Nevertheless, as birds are professionally skillful manipulators of air, it is reasonable to speculate that they might attain stabilized vision through aerodynamic interactions with the air. In this work we experimentally demonstrate that a hovering passerine exploits a unique aerodynamic trick to facilitate the stabilization of its eyes during downstroke.

To conduct the experiments, we trained eight passerines (Japanese White-eyes, *Zosterops japonicus*, body length 9.8 ± 0.7 cm, wingspan 15.2 ± 1.2 cm, body mass 8.1 ± 0.7 g; mean ± s.d.) to execute spontaneously and freely hovering flight in a transparent experimental chamber [60 × 60 × 120 cm (height × width × depth)]. We employed two synchronized high-speed video cameras (X-Stream$^{\mathrm{TM}}$ Vision 5, IDT) with orthogonal viewing directions to capture consecutive images of a hovering bird at 1000 frames $\mathrm{s}^{-1}$.

We tracked the center of mass (c.m.), the bird's eye, and the trailing tip of the tail in a hovering bird. The location of c.m. was measured in a similar way employed in our previous work [5]. A self-developed image-analysis program (written in MATLAB, version 7.0, The Mathworks, Natick, MA) was used to track the coordinates of feature points of a bird in a stationary coordinate system *XYZ*. These feature points of a bird were connected as a rigid bar representing the simplified trunk of the bird; the locomotion of the bird's body could consequently be described as translation and rotation of the rigid bar. The velocity of the c.m. ($V_{\mathrm{c.m.}}$) and angular velocity ($\omega$) of the rigid bar were also calculated.

Images recorded with high-speed video cameras revealed that a hovering passerine was less stationary than what we saw with the naked eye. In contrast, a substantial swinging up of the body during downstroke was observed. This finding is expected because a hovering passerine must generate a lift force greater than its body weight during downstroke to compensate for the lack of lift production during the upstroke that is aerodynamically inactive [2].

A mechanism for recovering the body posture was also observed. The bird's body seems to stop swinging up at the end of the downstroke; during the upstroke period, the bird's posture gradually recovers to the original state. However, this recovery mechanism remains mostly unclear at present. This report focuses on how a hovering passerine attains stabilized vision during downstroke.

Although a bird's body swings up substantially during downstroke, the bird's eyes are nearly stable (see Fig. 1): The bird's body appears to rotate about the eye. From a kinematic perspective, the eye is identified as the instant center of rotation of the bird's body. The evaluated displacements of the eye, the c.m., and the tail trailing tip for a single downstroke were 0.41 ± 0.15 cm, 2.35 ± 0.34 cm, and 4.79 ± 0.95 cm (mean ± s.d., $N = 16$), respectively. The ratio of the eye displacement to the tail trailing-tip displacement is ∼1/12, indicating that the passerine is able to inspect the environment stably even while its body is undergoing a substantial swing. In a statistical sense, no significant differences in displacements were observed among each passerine [assessed by one-way analysis of variance (ANOVA) followed by Student–Newman-Keuls test].

The results of the analysis of locomotion kinematics were insufficient to enable one to deduce how the hovering passerine maintains its eyes stationary in midair; we thus also quantitatively visualized and analyzed the fields of air flow produced by the passerine. Many accounts of bird flight have been devoted to the dissection of the downstream wake behind or beneath a flying bird, because the downstream wake represents the aerodynamic footprint of a flying animal [6,7]. Instead of the downstream wake, we focused on the transient variation of the near-wing wake flow fields generated during the downstroke. The reason is that, to stabilize its eyes against a swinging body during downstroke, a hovering passerine must be capable of performing some aerodynamic trick that is likely

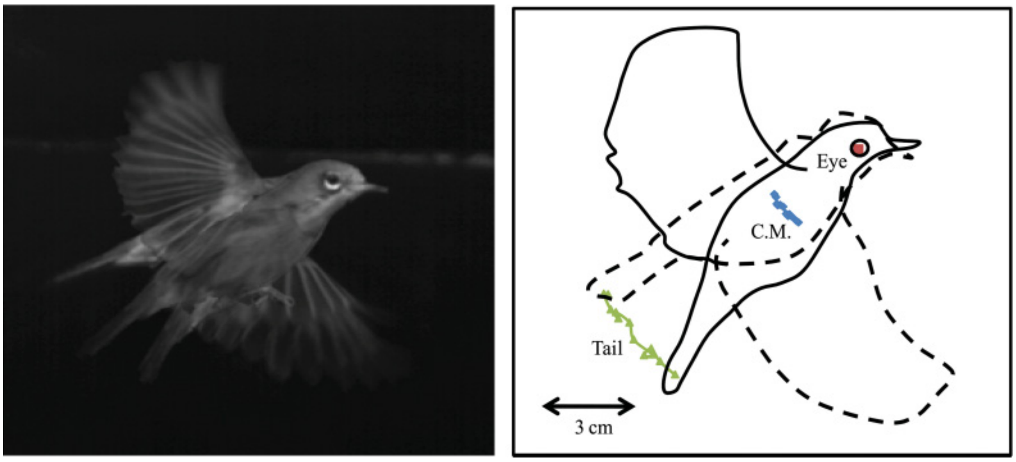

FIG. 1. (Color online) Image and schematic sketch illustrating the phenomenon of stabilized eyes during downstroke in a hovering passerine. The left panel shows an image produced by overlapping three consecutive images in the hovering passerine. In the right panel, the solid and dashed lines respectively refer to the outlines of the passerine for its initial and eventual postures of the downstroke. The sequential colored markers denote respectively the instant positions of the eye, c.m., and the tail trailing tip during downstroke.

to be revealed through scrutinizing the near-wing wake flow fields.

We employed two-dimensional digital particle-image velocimetry (DPIV) (Insight 3G, TSI Inc.) to visualize quantitatively the flow fields generated by a hovering passerine [Fig. 2(a)]. The DPIV seeding particles tracing the flow motion were illuminated with a sheet of light from a laser. The DPIV camera recorded the flow motion on the light sheet, and the motion camera simultaneously recorded the locomotion of the bird for kinematic analysis (1000 frames $s^{-1}$, image resolution of 1024 × 768 pixels). The size of the interrogation window used for DPIV analysis was 32 × 32 pixels, with 50% overlap of the interrogation window complying with the Nyquist criterion. The detailed procedure for the DPIV flow-field analysis was similar to that in our previous work [8]. As the passerine was hovering spontaneously without physical constraint, numerous experimental trials were undertaken; only those trials in which the parasagittal plane of the passerine was parallel to the light sheet were selected [Fig. 2(b)] for further analyses.

The flow fields induced by a hovering passerine during downstroke are shown in Fig. 3(a) in chronological order. A pair of counterrotating vortices were observed, indicating that the passerine induced a strong downward air jet during downstroke [9]. In the literature on the fluid mechanics of animal locomotion, such a flow configuration comprising a pair of counterrotating vortices and a central fluid jet is widely reported, signifying production of a locomotor force. The air jet generated by the downstroking bird wings might be a crucial factor contributing to the vision stabilization of the bird.

To characterize the air jet, we employed a $\lambda_2$ method [10,11] to identify precisely the positions of the cores of the counterrotating vortices. The $\lambda_2$ method is widely used in fluid mechanics to accurately detect and identify the cores of vortices distributed in a flow field [11]. $\lambda_2$ is defined as the second largest eigenvalue of a symmetric tensor $S^2 + \Omega^2$, where $S$ and $\Omega$ are, respectively, the symmetric and antisymmetric parts of the velocity gradient tensor $J$, with $J = S + \Omega$, $S = (J + J^{\mathrm{T}})/2$, and $\Omega = (J - J^{\mathrm{T}})/2$. For flow fields quantified with DPIV on a two-dimensional plane, $\lambda_2$ becomes

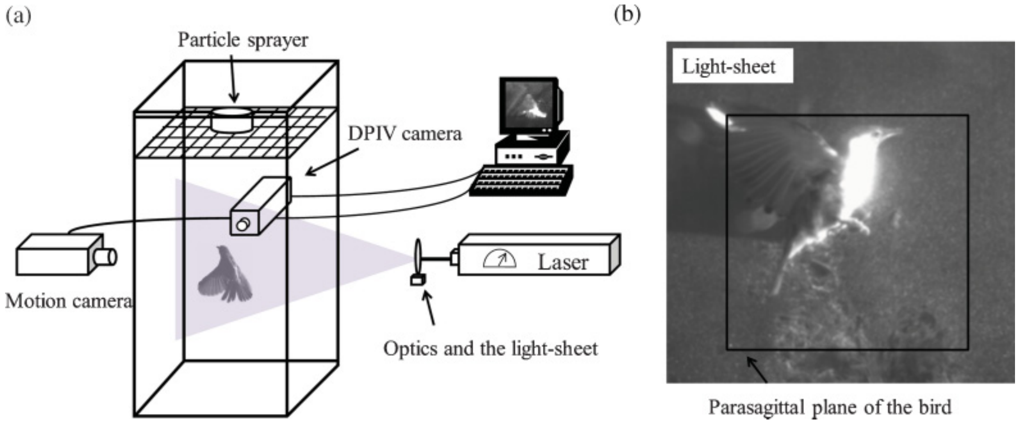

FIG. 2. (Color online) (a) Schematic illustration of the experiment for DPIV measurement. (b) Photograph taken by the DPIV camera on the parasagittal plane parallel to the light sheet.

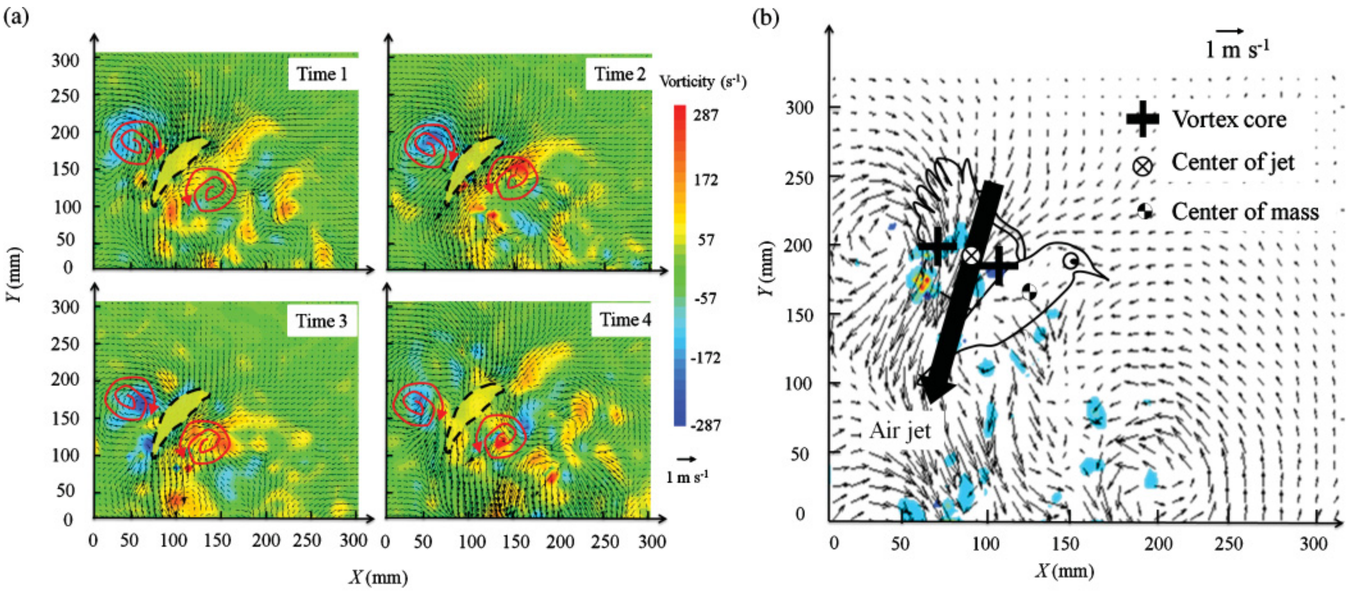

FIG. 3. (Color online) Flow-field snapshots of a hovering passerine acquired via DPIV during downstroke. (a) Velocity-vector plot and vorticity distribution of the flow fields. Data are shown at four consecutive stages (times 1–4). The outline of the bird body (shaded yellow) is marked with a dotted black line; red spirals with arrows denote the counterrotating vortices and their rotating direction. (b) Velocity-vector plot of a flow field. The color contour represents the distribution of $\lambda_2$. The blue patches indicate regions subjected to negative values of $\lambda_2$. The thick black arrow denotes the position and orientation of the strong air jet generated by the downstroking wings.

simplified to

$$\lambda_2 = \left(\frac{\partial u}{\partial x}\right)^2 + \left(\frac{\partial u}{\partial y}\right)\left(\frac{\partial v}{\partial x}\right), \qquad (1)$$

where $u$ and $v$ are, respectively, the fluid velocities along the $x$ and $y$ axes of the flow measurement plane. For a measured flow field, a point subjected to a negative minimum of $\lambda_2$ is identifiable as a vortex core, because the swirling motion is locally stronger than the shearing motion. The midpoint between the identified cores of a pair of counterrotating vortices is considered to be the center of the air jet.

In total, 26 sequences of bird flow fields were analyzed to determine the position of the air-jet center with respect to the c.m. of the bird. The cores of counterrotating vortices were identified on inspecting the $\lambda_2$ contours [Fig. 3(b)]. For a hovering passerine, the air-jet center is invariably located dorsal to the c.m., i.e., on the back side [Fig. 3(b)], with a spatial deviation 0.55–2.67 cm from the c.m. The orientation of the air jet was assumed to be identical to that of the streamlines situated at the air-jet center, which was pointed mostly downward.

According to Newton's second and third laws of motion, as the bird accelerates the air jet downward, a lifting reaction force is experienced by the bird. As the air jet is produced dorsal to the c.m. during downstroke, the position of action of the lifting force is also dorsal to the c.m. The production of this dorsal lifting force is considered to account for the aerodynamic trick employed by a hovering passerine to attain visual stabilization during downstroke.

One can reasonably infer that the stabilized vision results entirely from the cancellation of opposing displacements arising from the dorsal lifting force because there is no external constraint imposed on the bird's head or eyes. In Fig. 4, a free-body diagram for force analysis is presented, in which the bird's body is simplified as a rigid bar. During downstroke, the hovering passerine acquires a lifting force $F$ acting posteriorly to the c.m., concurrently producing both translation and rotation of the bird's body. $V_{\mathrm{c.m.}}$ and $\omega$ represent, respectively, the translational and rotational (i.e., angular) velocities of the bird's body.

For the body translation depicted in Fig. 4, the entire bird's body, including the eye, is inclined to become uplifted along the direction of $V_{\mathrm{c.m.}}$, but the body rotation (clockwise in Fig. 4) concurrently tends to displace the eye along the direction of $V_e$ $(=\omega \cdot r_1)$, which is opposed to $V_{\mathrm{c.m.}}$. In sum, there exist two velocity components, $V_{\mathrm{c.m.}}$ and $V_e$, at the eye, respectively pertaining to body translation and rotation. As the bird's eye is

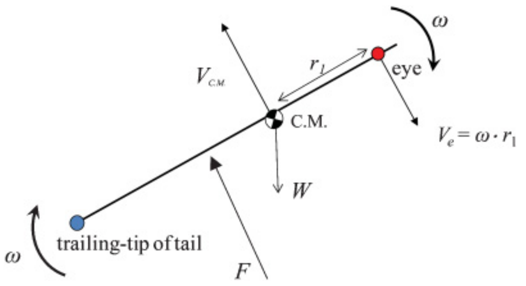

FIG. 4. (Color online) A free-body diagram for force analysis on a hovering bird during downstroke, with the bird's body being simplified as a rigid bar. $F$ is the air reaction force generated during downstroke, which simultaneously results in a body translation velocity $V_{\mathrm{c.m.}}$ and a body rotation with angular velocity $\omega$. $r_1$ is the distance between the eye and the c.m., and $W$ is the body weight.

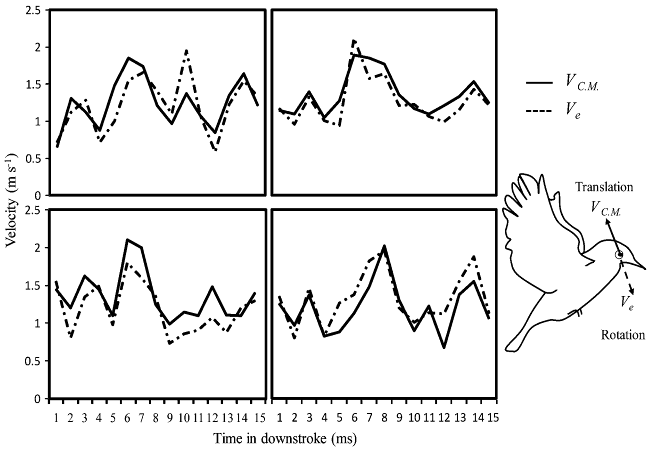

FIG. 5. Four representative samples (taken from four different individuals) illustrating the variation of $V_{\text{c.m.}}$ and $V_e$ during downstroke. The sketch to the right illustrates how opposing displacements associated with $V_{\text{c.m.}}$ and $V_e$ cancel at the eye.

spatially stabilized, the two opposing displacements stemming from body translation and rotation must cancel each other.

To examine the adequacy of our postulate, we evaluated both $V_{\text{c.m.}}$ and $V_e$ from the recorded images. In Fig. 5, we show four representative cases of the evaluated $V_{\text{c.m.}}$ and $V_e$; for the sake of conciseness, only the data for the preceding 15 ms of the downstroke duration are shown. $V_{\text{c.m.}}$ and $V_e$ have evidently the same order of magnitude, with an average deviation 11.3%. Moreover, the trend of variation of the magnitudes of $V_{\text{c.m.}}$ and $V_e$ is approximately consistent during downstroke. These findings support the idea that, for the bird's eye, the opposing displacements associated with $V_{\text{c.m.}}$ and $V_e$ continuously cancel each other.

Provided that the lifting force generated during the downstroke passes exactly through the c.m., only a body translation results; in this situation, an eye displacement is inevitable because a required opposing displacement vanishes. For flights at large flapping frequencies (e.g., 24 Hz in a hovering passerine), stable vision is extremely important for a bird to inspect the environment [12]. Our experiments reveal that, to resolve such a problem, a passerine generates a lifting force dorsal to the c.m., causing a body motion with two degrees of freedom—translation and rotation. Counterintuitively and intriguingly, such a complicated body motion does not deteriorate the stability of the eye; the eye remains, instead, stabilized because the displacement due to body translation becomes offset by the displacement due to body rotation. This condition also notably renders a displacement of the eye only 8% that of the trailing tip of the tail.

In addition to the aerodynamic trick revealed in this report, there exist some other means by which a bird stabilizes its head and eyes. The neck muscles and skeleton, as physiological mechanisms, are reported [3] to function as a damping system to diminish the head instability caused by external perturbations applied to a bird. The aerodynamic trick we addressed here is deemed useful and efficient particularly for high-frequency flapping flight because this trick stabilizes the eye directly by mutual cancellation of two opposing displacements, rather than by the damping effects. However, our findings suggest that physiological mechanisms can be jointly employed with the aerodynamic trick to facilitate visual stabilization in a bird. For instance, the aerodynamic trick we proposed in this report ensures the stabilization of the bird's eye but does not guarantee the stabilization of gaze because the eye may still rotate even if it remains located in a fixed spatial point. Actually, not only the stabilization of the eye but also the stabilization of gaze was observed in a hovering passerine. This stabilization of gaze is probably maintained by a physiological mechanism called "vestibulo-ocular reflex" that has been reported in avian literature [13,14]. That is, a flapping bird is likely to be equipped with more than one system to stabilize its vision, and various systems collaborate to stabilize the vision in an efficient manner.

Based on a mechanical perspective, this work provides insight into how a hovering bird attains stabilized vision during downstroke. This aerodynamic trick for visual stabilization offers bioinspired guidance for engineers to enhance the visual stability of surveillance cameras incorporated in micro aerial vehicles (MAV).

The National Science Council of the Republic of China partially supported this work under Contracts No. NSC 96-2628-E-002-256-MY3 and No. NSC 96-2628-E-002-258-MY3. The authors would like to thank the editors and two anonymous reviewers for providing helpful comments on this paper.

---

[1] B. W. Tobalske, Physiol. Biochem. Zool. **73**, 736 (2000).

[2] U. M. Norberg, *Vertebrate Flight: Mechanics, Physiology, Morphology, Ecology and Evolution* (Springer-Verlag, Berlin, New York, 1990), pp. 99–117.

[3] B. J. Frost, Curr. Biol. **19**, R315 (2009).

[4] G. Katzir, E. Schechtman, N. Carmi, and D. Weihs, J. Comp. Physiol. A **187**, 423 (2001).

[5] S. C. Ting and J. T. Yang, J. Exp. Biol. **211**, 3147 (2008).

[6] J. J. Videler, in *Avian Flight* (Oxford University Press, Oxford, New York, 2005), pp. 116–180.

[7] J. O. Dabiri, J. Exp. Biol. **208**, 3519 (2005).

[8] Y. H. Chang, S. H. Ting, C. C. Liu, J. T. Yang, and C. Y. Soong, Exp. Fluids (2011).

[9] H. J. Lugt, in *Vortex Flow in Nature and Technology* (Krieger, Malabar, FL, 1995), pp. 18–40.

[10] S. C. Ting and J. T. Yang, Phys. Fluids. **21** (2009).

[11] J. Jeong and F. Hussain, J. Fluid. Mech. **285**, 69 (1995).

[12] J. D. Dickman and I. Lim, J. Assoc. Res. Otolaryngol. **5**, 323 (2004).

[13] J. Wallman, J. Velez, B. Weinstein, and A. E. Green, J. Neurophysiol. **48**, 952 (1982).

[14] A. Haque and J. D. Dickman, J. Neurophysiol. **93**, 1165 (2005).